Astron. Astrophys. 321, 625–633 (1997)

ASTRONOMY
AND
ASTROPHYSICS

Thermal methanol emission in the DR 21 complex

Interferometric maps: a comparison with maser emission

S. Liechti[1] **and C.M. Walmsley**[2,3]

[1] Centro Astronómico de Yebes (IGN), Apartado 148, E-19080 Guadalajara, Spain
[2] I. Physikalisches Institut, Universität zu Köln, Zülpicherstr. 77, D-50937 Köln, Germany
[3] Osservatorio Astrofisico di Arcetri, Largo E.Fermi 5, I-50125 Firenze, Italy

Received 22 July 1996 / Accepted 22 October 1996

Abstract. We present interferometric observations with $\sim$3.5″ resolution of the $2_k \rightarrow 1_k$ methanol lines towards the methanol masers in the DR 21/DR 21(OH) complex. These transitions are not masing and hence our measurements can be used to place limits on the methanol mass associated with the maser spots. We do not find in general good correlation between the peaks of "non-maser" methanol emission and the positions of Class I methanol masers. In particular, we put an upper limit on $2_k \rightarrow 1_k$ emission towards the $8_0 \rightarrow 7_1A^+$ maser DR 21(OH)-1 from Plambeck and Menten (1990) (hereafter PM90). We do find however evidence for coincidence between the peak of the $2_1 \rightarrow 1_1E$ emission in our map with the Class I masers towards DR 21-W. We conclude that methanol Class I masers are likely to originate in a region considerably smaller than our synthesised beam (3.5″) and with methanol column density of order 10^{16} cm^{-2}. It seems reasonable that they might form in regions of diameter 1000 AU and mass 0.01 $M_\odot$. Our data also show differences between the distribution of methanol and that of other species which suggest large spatial variations in the methanol abundance. In particular, we see evidence for high methanol column density towards the submillimeter continuum source DR 21(OH)-MM1.

In the western lobe of the DR 21 outflow, the thermal methanol emission appears to be "sandwiched" between vibrationally excited H_2 emission, tracing the outflow shock front, and CS emission tracing the dense ambient medium. This is consistent with the idea that methanol can be enhanced in shock regions, where the outflow impinges on the surrounding dense molecular clumps, releasing methanol from dust grain ice mantles.

Key words: ISM: molecules – ISM: individual objects: DR 21; DR 21(OH) – Radio lines: ISM – stars: formation

Send offprint requests to: C.M. Walmsley

1. Introduction

The Class I methanol masers, although located in massive star forming regions, are generally found offset (sometimes by more than 1 pc) from the typical tracers of newly formed stars: ultracompact H II regions, strong infrared sources, OH and H_2O masers (see e.g. Menten 1991, Liechti & Wilson, 1996). Both single dish and interferometric measurements (Menten 1991) have shown that the different Class I maser transitions (at 25, 36, 44, 84 and 95 GHz) arise from the same spot, which suggests that similar conditions are needed to produce all these lines. Indeed, it seems reasonable that a collisional pump is operating and statistical equilibrium calculations show that the 36, 44, 84 and 95 GHz maser lines will have inverted populations at densities of around 10^6 cm^{-3} and temperatures of 50–100 K (Liechti & Wilson, 1996). The mass and size of the regions giving rise to Class I methanol maser emission are however unclear. A related problem is whether the methanol Class I maser clumps can be detected in non-maser emission. If so, one has the possibility of determining the parameters of these regions in a manner unaffected by the vagaries of maser emission. If not, one can at least place limits on the characteristics of the masers. The objective of the present set of observations was to use observations of the quartet of J=2→1 a-type methanol lines around 96.7 GHz for this purpose. The 96.7 GHz lines have been observed in various star-forming regions (e.g. Gottlieb et al. 1979, Menten et al. 1988) and do not show maser action. Nor is Class I maser action in these transitions expected from theoretical arguments. Moreover, the measured relative intensities of different $J_k \rightarrow (J-1)_k$ transitions can be roughly fit with a Boltzmann population distribution (not in general thermal) which is a characteristic of non-maser emission. With this in mind, we undertook measurements of the 96.7 GHz $2_k \rightarrow 1_k$ methanol lines towards the well studied methanol masers in DR 21/W 75S.

The DR 21/W 75S region is one of the few molecular complex for which interferometric observations of Class I methanol masers have been published (Batrla & Menten 1988; Plambeck & Menten 1990, hereafter PM90). Moreover, this well stud-

ied star forming region located in the Cygnus X complex at a distance of about 3 kpc (Dickel et al. 1969) has been mapped in many frequencies and molecular lines; both the DR 21 H II region with its associated massive outflow (see e.g. Garden et al. 1991 and Garden & Carlstrom 1992) and the younger star forming region 3′ north, DR 21(OH) (see e.g. Mangum et al. 1991, Mangum et al. 1992). The complete region has also been mapped with resolutions between 12 and 40″ in $C^{18}O$, $C^{34}S$ and NH_3 by Wilson & Mauersberger (1990).

The interferometric observations of PM90 show that the DR 21-W methanol maser is located between the CS emission peaks and the excited molecular hydrogen emission. The authors suggest that methanol masers are formed in clumps where molecular outflows interact with pre-existing ambient gas: the heating produced by the shock may cause an increase in methanol abundance (e.g. by evaporation of methanol ice condensed on dust grains), favoring the formation of collisionally pumped methanol masers. High resolution observations of thermal methanol in the same regions can help quantify this hypothesis.

This paper presents interferometric observations of the group of the $2_k \rightarrow 1_k$ methanol transitions in two fields; one around DR 21(OH) where four $8_0 \rightarrow 7_1 A^+$ methanol masers (DR 21(OH)-1 – 4) have been detected (PM90), and the second around the bright methanol maser DR 21-W in the western lobe of the DR 21 outflow. In Sect. 2, we give details of our observations and in Sect. 3, we summarize the main observational results. In Sect. 4, we discuss the consequences of our results for methanol maser models and in Sect. 5, we give our main conclusions.

2. Observations

Observations of the $2_k \rightarrow 1_k$ methanol line quartet were acquired in June and September 1993, with three configurations of the IRAM Plateau de Bure 4-element interferometer (Guilloteau et al. 1992).

The four 15-m dishes were equipped with SIS receivers having double-sideband temperatures of 50–100 K. The CD configuration with baselines between 24 and 176 meters was used. The two fields, one centered on DR 21-W, the strong methanol maser in the western lobe of the DR 21 outflow (α_{1950} = $20^h37^m07.82^s$, δ_{1950} = 42°08′44.6″) and the other centered on DR 21(OH)-2 (see PM90, α_{1950} = $20^h37^m13.23^s$, δ_{1950} = 42°12′08.6″) were observed simultaneously spending one fifth of the time on the DR 21(OH) field, since the line intensities in DR 21(OH) were expected to be much stronger than in DR 21-W. The amplitude and phase calibration were carried out with frequent observations of the nearby quasar 2005+403. A typical observing cycle was 4 minutes on the calibrator, 4 minutes on the DR 21(OH) field and 16 minutes on the DR 21-W field. The flux of 2005+403 was estimated from observations of one or two of the strong flux calibrators regularly monitored by the PdBI team and was found to be fairly constant between June and September 1993 with a value of 1.15 Jy at 96.7 GHz. This value is in good agreement with independent flux measurements with the IRAM 30 meter radiotelescope (see e.g. Steppe et al. 1993).

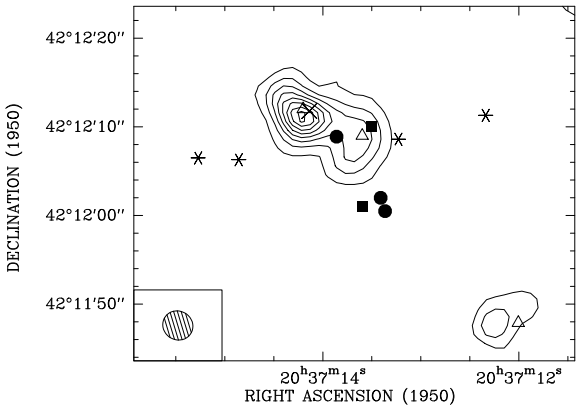

Fig. 1. CLEANed map of the 3.1mm continuum emission towards DR 21(OH). Contours are drawn in steps of 10 mJy/beam starting at 10 mJy/beam. We have corrected for primary beam attenuation. The 3.5″ × 3.2″ beam is drawn in the bottom left corner. Indicated are the positions of the $8_0 \rightarrow 7_1 A^+$ methanol masers (Stars; PM90), the H_2O maser groups (Filled circles; Mangum et al. 1992), the OH maser (Cross; Norris et al. 1982), the H_2CO emission peaks (Filled square; Johnston et al. 1984) and the 2.7mm continuum emission peaks (Unfilled triangles; Mangum et al. 1991).

The four methanol lines were observed using two spectral line correlator units with 256 channels covering 20 MHz each, giving a channel separation of 78kHz, which corresponds to 0.24 kms^{-1}. The effective spectral resolution is about 1.3 times coarser. The first correlator band was centered at the rest frequency of 96.742 GHz and a V_{LSR} of -2.6 kms^{-1} in order to encompass the $2_{-1} \rightarrow 1_{-1}$E, the $2_0 \rightarrow 1_0 A^+$ and the $2_0 \rightarrow 1_0$E methanol transitions, and the second, 15 MHz higher to observe the $2_1 \rightarrow 1_1$E transition. Three other correlator units covering 160 MHz each, were used to cover the whole baseband. To avoid line contamination, only the two extreme units were used to derive the continuum emission.

The reduction was carried out using the CLIC and GILDAS software packages developed at IRAM and the Observatoire de Grenoble. The CLEAN algorithm applied to the u-v data with uniform weighting, and no taper, gives a gaussian clean beam of approximately 3.5″ × 3.2″ (pos.angle 65°) for the continuum and 3.8″ × 3.1″ (pos.angle 45°) for the spectral line data. The telescope primary beam is about 51.2″ at λ =3.1 mm.

For the line data, gaussians have been fitted to the resulting spectra for each pixel of the maps. In this way, we have derived the integrated area, center velocity and line width for each methanol transition. Fig. 1 shows the continuum emission in DR 21(OH) and Fig. 2, the resulting maps of the line integrated area for each methanol transition towards both fields.

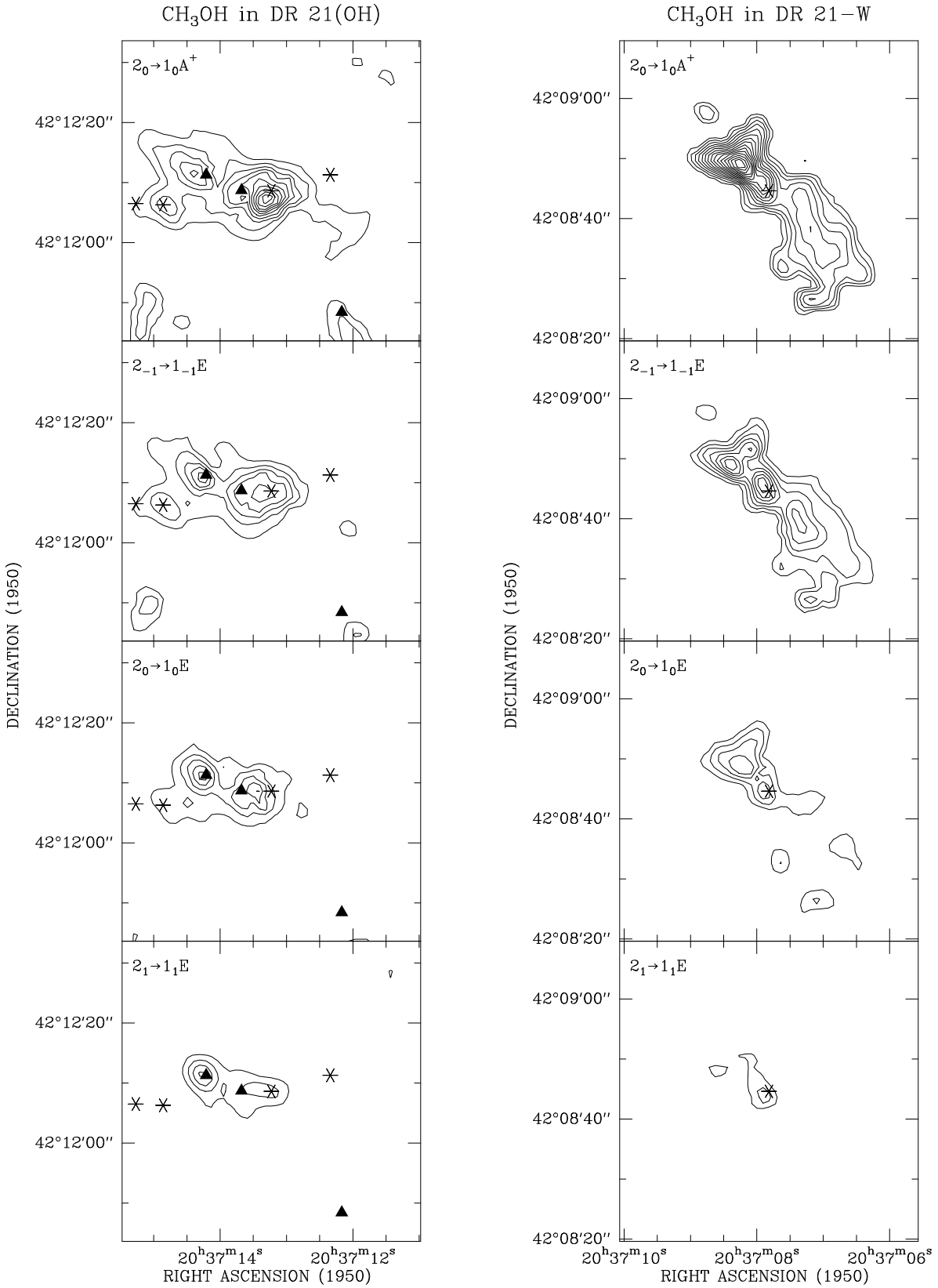

Fig. 2. Contour maps of the methanol integrated intensity (resulting from gaussian fits) in each transition. The levels are from 0.5 to 6 Jy.kms^{-1} in steps of 0.5 Jy.kms^{-1} for DR 21(OH), and from 0.1 to 1.7 Jy.kms^{-1} in steps of 0.1 Jy.kms^{-1} in DR 21-W The stars mark positions of $8_0 \rightarrow 7_1A^+$ methanol masers from PM90, and the filled triangles, the positions of the continuum emission peaks derived from our observations (Table 1).

Table 1. Parameters of 3.1mm continuum components in DR 21(OH).

Components	α_{1950} [1,2]	δ_{1950} [1,2]	$\theta_{maj} \times \theta_{min}$ [1,3]	Pos. angle[1,4]	Integrated Flux (Jy)
MM1	20h 37m 14.21s	42° 12′11.3″	6.6″ × 4.6″	52°	0.22±0.02
MM2	20h 37m 13.66s	42° 12′08.3″	7.8″ × 5.9″	158°	0.15±0.01
DR 21(OH)W	20h 37m 12.17s	42° 11′48.4″	6.5″ × 4.5″	128°	0.07±0.01

[1] Determined from spatial 2-dimensional gaussian fit. The sizes of the clumps are not corrected for the synthesised beam. [2] Error in the positions is 0.1″. [3] Error in angular sizes is estimated to be 0.2″. [4] Error in position angle is estimated to be 4°.

3. Results

3.1. Continuum emission

Fig. 1 shows the 96.7 GHz continuum emission map towards DR 21(OH). It is very similar to the map of Woody et al.(1989) at 1.4 mm with the two sources MM1 and MM2 clearly present. The RMS noise on the map is 1.5 mJy/beam. The weak peak to the south-west corresponds to the DR 21(OH)W source observed by Mangum et al.(1991) at 2.7 mm. The results from a gaussian fit to the three sources are listed in Table 1. We note that with our improved angular resolution, MM1 appears more compact and brighter than MM2 (83 mJy/beam as opposed to 37 mJy/beam; 1 K = 91 mJy/beam). Moreover, the peak is 0.7″ to the south of that found by Mangum et al. and 1.7″ to the south of the 1.3 mm maximum of Woody et al.(1989). This suggests the presence of a compact component but higher angular resolution measurements are needed to confirm this. Our fluxes for MM1 and MM2 are about 20 percent higher than expected on the basis of extrapolating the results of Mangum et al.(1991) to lower frequencies using the dust emissivity index (1.7) proposed by them. Given the small frequency baseline and possible calibration errors, this difference is not significant.

Our DR 21-W field was centered about 75″ west from the strong continuum source DR 21, a group of compact HII regions. Although it is located three times further than the half power level of the primary beam, this source is so strong that it greatly contaminates the continuum map. We applied the CLEAN algorithm to a 1024″ × 512″ map so as to cover properly the DR 21 continuum source. The resulting map with a noise level of about 0.8 mJy per beam shows a group of sources aligned north to south around the location of the DR 21 continuum source. No emission is detected around the DR 21-W maser position down to a limit of 2.5 mJy/beam.

3.2. Methanol emission

3.2.1. DR 21(OH)

Our DR 21(OH) field encompasses the four methanol masers detected by PM90 at 95 GHz, and was centered on DR 21(OH)-2 about 5″ west of MM2. Our integrated intensity maps are shown in Fig. 2 and 3. They show a clumpy structure extended along the same axis as MM1 and MM2. There is no obvious correlation between the peaks on our maps and the 95 GHz $8_0 \rightarrow 7_1A^+$ maser spots from PM90. In fact, towards the strongest (western) 95 GHz maser, DR 21(OH)-1, we observe no emission in the $2_k \rightarrow 1_k$ series down to an upper limit of 164 mJy/beam (1.8 K). DR 21(OH)-2 however is only ∼1″to the north-west of the strongest peak in $2_0 \rightarrow 1_0A^+$ and DR 21(OH)-4 coincides well with a peak in "non-maser" methanol emission. Thus, while there may be a relationship between "maser" and "non-maser" methanol, it must be of an indirect nature.

It is also interesting that our maps in $2_k \rightarrow 1_k$ methanol emission have a different morphology to those observed in other species such as $C^{18}O$ (Mangum et al. 1991), ammonia (Mangum et al. 1992), or CS (PM90). The methanol emission is oriented along a northeast-southwest axis (position angle of about 70° east of north). We detect emission towards the south-western continuum emission component DR 21(OH)W and also to the south-east (perhaps related to the south-east CS clump of Richardson et al. 1994).

There are clear excitation effects visible on our maps (Fig. 2). The $2_1 \rightarrow 1_1E$ line for example is expected to be emitted in hotter and denser regions than the other three. Fig. 2 shows that while the strongest peak in $2_0 \rightarrow 1_0A^+$ is close to the PM90 maser DR 21(OH)-2, the strongest peak in $2_1 \rightarrow 1_1E$ is close to MM1 (0.7″away). Qualitatively, this suggests that the hottest densest gas in the region is close to MM1.

In order to have a quantitative measure of the parameters of the methanol clumps, we have used 2-dimensional gaussian decomposition to derive characteristics of the "cores" which we detect. The results of this are given in Table 2 where we list positions and sizes derived from fits to the $2_0 \rightarrow 1_0A^+$ map. From spectra towards clump maxima, we have obtained the intensities, velocities, and line widths listed in Table 2. The integrated line intensities obtained in this way were used to derive column densities in the lower levels of the observed transitions under the assumption that the lines are optically thin and that the excitation temperatures are much higher than the cosmic background (see discussion of Menten et al. 1988). Finally, a fit of the level column densities derived in this manner to a Boltzmann distribution allowed us to obtain the total column densities and rotation temperatures given in Table 2 (Eq. 4 of Menten et al., 1988).

Fits of this type can be misleading for a number of reasons (see discussion of MM1 in Sect. 4.1). In the first place, experience shows that the low optical depth assumption is often not valid. In such cases, the derived level column densities will be underestimated and there is usually a tendency to overestimate

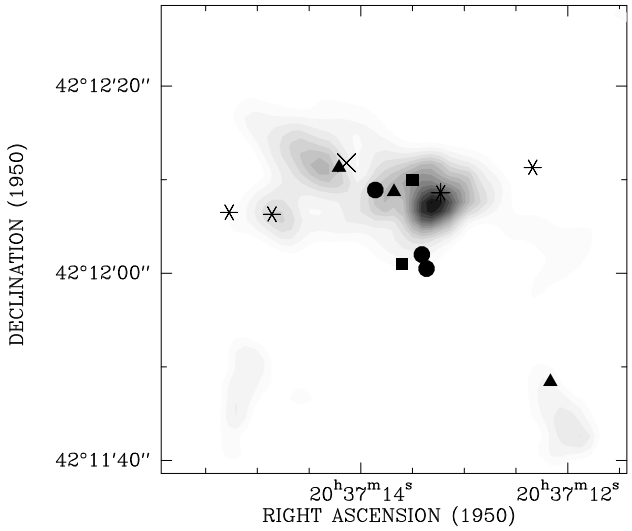

Fig. 3. Map of the $2_0 \rightarrow 1_0A^+$ methanol transition emission in DR 21(OH). The grey-scale map shows the integrated intensity of this transition in steps of 0.3 Jy kms^{-1} starting at 0.5 Jy kms^{-1}. The symbols are the same as the ones used in Fig. 1, except that the continuum emission peaks are the ones derived from the observations reported in this paper (Table 1), and are indicated by filled triangles.

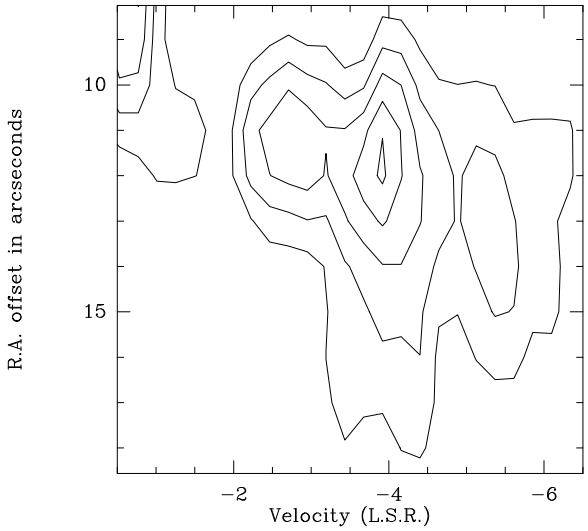

Fig. 4. Velocity-position plot of the $2_0 \rightarrow 1_0A^+$ methanol transition in MM1. The cut is along the right ascension axis and the emission was summed over declinations 42°12′09.6″ to 42°12′12.6″. The ordinate axis is in right ascension arcseconds offset from the field center.

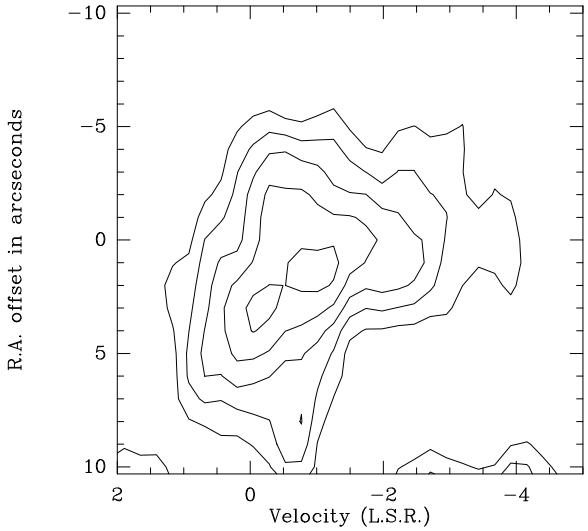

Fig. 5. Velocity-position plot of the $2_0 \rightarrow 1_0A^+$ methanol transition around DR 21(OH)-2. The cut is along the right ascension axis and the emission was summed over declinations 42°12′07.6″ to 42°12′12.6″. The ordinate axis is in right ascension arcseconds offset from the field center.

$T_{\rm rot}$. Also, statistical equilibrium calculations (e.g. Menten et al. 1988) show that for typical molecular core densities (see also Bachiller et al. 1995), methanol level populations are very sub-thermal and far from LTE. In these circumstances, a fit to a Boltzmann distribution will result in $T_{\rm rot}$ estimates which are small compared to the kinetic temperature. Nevertheless, such a fit allows a useful parametrisation of the data and shows, for example, that MM1 has much higher excitation than all other cores. We conclude also from Table 2 that in all cores except MM1, either the temperatures or densities or both are low (T below 50 K and n(H_2) below 10^7 cm^{-3}). Deciding which of these is the case requires a comparison with a temperature-sensitive tracer such as ammonia. In a couple of cases, comparison with the data of Mangum et al. (1992, e.g. MM2 and DR 21(OH)W-A) suggests that the core kinetic temperatures are of order 30 K and thus that, as expected, methanol is very sub-thermally excited.

Each of the continuum emission components described in Sect. 3.1 appears to be associated with $2_k \rightarrow 1_k$ methanol emission although the latter typically has a maximum slightly offset from the continuum emission peaks. Clump 4 (see Table 2), which peaks close to DR 21(OH)-4, may be associated with the -5 kms^{-1} pedestal emission component detected at 95 GHz between the maser spots DR 21(OH)-3 and DR 21(OH)-4 (see PM90), which suggests a thermal origin for this pedestal 95 GHz emission. Also, clump 7 may correspond to the W-A NH_3 core of Mangum et al. (1992).

The velocity shift in MM1 along the right ascension axis detected by Mangum et al. (1992) in ammonia is also clearly visible in methanol. We show this in Fig. 4 which is a velocity-offset plot of the $2_0 \rightarrow 1_0A^+$ line in the right ascension direction. One sees that the linewidth becomes larger towards MM1 and that blue shifted emission is predominant to the east.

There is also a velocity shift along the right ascension axis but in the opposite direction (with velocity decreasing to the west) around the first methanol clump of Table 2, which is very close to the maser DR 21(OH)-2 of PM90. Thus there could be a weak outflow around this maser (Fig. 5). However, since MM2 is also in the vicinity, one could be observing two different clumps with different velocities. One of these might be associ-

Table 2. Parameters of the methanol cores associated with DR 21(OH).

Components	α_{1950}[1]	δ_{1950}[1]	$\theta_{maj} \times \theta_{min}$[1]	Pos. angle[1]	v_{lsr} kms^{-1}	Δv kms^{-1}	T_{rot}[2] K	$N(CH_3OH)$[2] 10^{15} cm^{-2}
1 (DR 21(OH)-2)	20h 37m 13.27s	42° 12′08.0″	8.1″ × 6.5″	110°	−1.1	3.2	14±5	5.0±3.1
2 (MM2)	20h 37m 13.45s	42° 12′08.4″	9.6″ × 7.8″	45°	−0.2	3.5	18±5	5.3±3.2
3 (MM1)	20h 37m 14.28s	42° 12′11.2″	5.4″ × 4.3″	58°	−3.4	3.5	74±52	38±45
4 (DR 21(OH)-4)	20h 37m 14.78s	42° 12′05.0″	7.3″ × 4.4″	46°	−5.1	2.5	11±1	2.1±0.4
5	20h 37m 13.55s	42° 12′03.0″	9.3″ × 5.3″	84°	−0.8	1.8	13±1	1.7±0.4
6	20h 37m 15.15s	42° 11′47.7″	5.1″ × 3.2″	135°	−2.4	1.9	8±2	0.8±0.5
7 (DR 21(OH)W-A)	20h 37m 12.09s	42° 11′45.0″	10.6″ × 5.0″	45°	−1.9	1.7	11±4	0.8±0.5
8	20h 37m 14.95s	42° 12′16.5″	6.3″ × 4.4″	53°	−3.9	2.0	9±3	0.7±0.4
9	20h 37m 12.00s	42° 12′02.6″	7.3″ × 5.6″	78°	−4.5	1.4	11±2	0.6±0.3
10	20h 37m 14.55s	42° 11′46.9″	3.7″ × 3.4″	46°	−3.7	1.2	9±5	0.5±0.4

[1] Determined from 2-dimensional gaussian fit to the integrated intensity map of the emission of the $2_0 \rightarrow 1_0A^+$ methanol transition. The size is not corrected for the synthesised beam. Errors on the positions are 0.3″ and on the angular sizes 0.6″
[2] Errors only include the statistical errors on the fit.

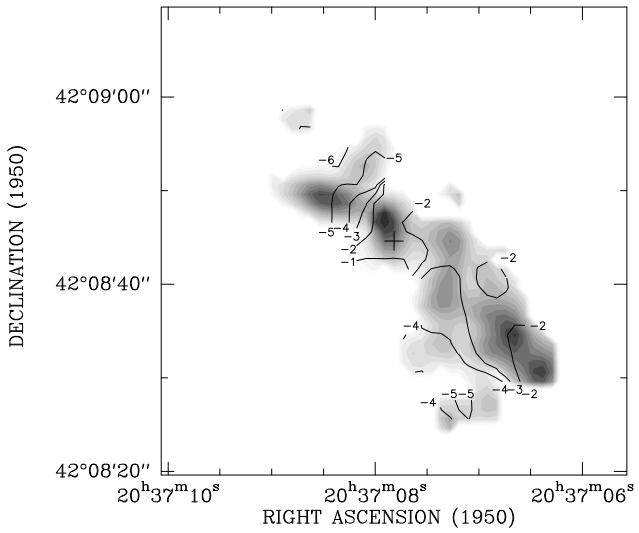

Fig. 6. Map of the $2_0 \rightarrow 1_0A^+$ methanol transition emission in DR 21-W. The grey-scale map shows the peak intensity (from gaussian fits) in steps of 0.025 Jy starting at 0.05 Jy. The contours show the center velocity in steps of 1 kms^{-1}, from −6 to −1 kms^{-1}.The maser position is shown by a cross.

ated with the MM2 continuum source (clump 2 in Table 2) and the other with the maser spot.

3.2.2. DR 21-W

Our DR 21-W field was centered on the strong methanol maser emission 75″ west of the DR 21 HII complex, mapped with the BIMA array at 95GHz by PM90. This maser lies on the northern edge of the western lobe of the DR 21 molecular outflow, between a clump of low velocity molecular gas and the high velocity molecular outflow (Garden and Carlstrom 1992).

The observed thermal methanol emission (see Fig. 2 and 6) is distributed in several clumps in an elongated structure surrounding the maser position and oriented north–east south–west. Their parameters are listed in Table 3 and have been derived in the same fashion as discussed for DR 21(OH) in the previous section. There is again evidence for a velocity gradient with more blue-shifted velocities to the north–east (see Fig. 6).

The rotation temperature diagram method gives rotational temperatures between 7 and 12 K and column densities of 0.2 10^{15} to 1.1 10^{15} cm^{-2} for the different clumps (Table 3). Fig. 2 shows that the peak of $2_1 \rightarrow 1_1$E emission is close to the maser position (0.8″ displaced) and so in this case, there is evidence for high density gas close to the maser position. Interferometric measurements in higher excitation non-maser transitions would be useful to investigate the significance of this. We can also get a crude estimate of the methanol column density associated with the maser emission under the assumption that the $2_1 \rightarrow 1_1$E emission observed by us is emitted by the maser clump and that the lower excitation transitions are emitted by surrounding more extended material. Then (see discussion in Sect. 4.2) for an arbitrarily assumed rotation temperature of 50 K, we estimate the methanol beam–averaged column density to be 2.1 10^{15} cm^{-2}. This is an upper limit in that there may be contributions to the observed $2_1 \rightarrow 1_1$E emission from gas surrounding the maser region but on the other hand we are assuming low optical depth in the $2_1 \rightarrow 1_1$E line which may lead to an underestimate.

4. Discussion

4.1. The MM1 source

It is clear from the results in Table 2 that the methanol spectrum towards the continuum source MM1 in DR 21(OH) is unusual. For this reason, we show the spectrum towards MM1 in Fig. 7. Line parameters derived from gaussian fits are given in Table 4. The peak line temperatures are close to being identical and equal to $\sim$ 9 K for the three lower excitation lines. Only $2_1 \rightarrow 1_1$E is somewhat weaker. As Table 2 makes clear, this situation is unusual in our data set and in fact, to our knowledge, only to-

Table 3. DR 21-W methanol emission cores characteristics.

Components	α_{1950}[1]	δ_{1950}[1]	$\theta_{maj} \times \theta_{min}$[1]	Pos. angle[1]	v_{lsr} kms^{-1}	Δv kms^{-1}	T_{rot}[2] K	$N(CH_3OH)$[2] 10^{15} cm^{-2}
1	20h 37m 07.89s	42° 08′46.2″	7.1″ × 5.1″	45°	−1.9	3.5	9±2	0.9±0.5
2[3]	20h 37m 07.88s	42° 08′44.4″	5.1″ × 3.4″	45°	−1.1	3.2	12±3	1.1±0.5
3	20h 37m 08.43s	42° 08′49.2″	8.3″ × 4.0″	79°	−5.3	3.2	8±3	0.7±0.4
4	20h 37m 06.72s	42° 08′34.2″	11.1″ × 6.2″	45°	−2.1	1.2	10±2	0.3±0.2
5	20h 37m 07.31s	42° 08′44.2″	5.8″ × 4.5″	66°	−2.7	1.9	7±2	0.3±0.2
6	20h 37m 08.12s	42° 08′52.3″	7.3″ × 3.6″	152°	−5.0	3.8	7±2	0.5±0.3
7	20h 37m 07.29s	42° 08′39.1″	14.2″ × 6.1″	177°	−3.3	2.3	6±3	0.3±0.2
8	20h 37m 06.45s	42° 08′31.2″	3.8″ × 3.5″	55°	−1.5	1.1	6±3	0.3±0.2
9	20h 37m 07.25s	42° 08′26.1″	3.7″ × 2.6″	123°	−5.0	2.8	8±2	0.4±0.2
10	20h 37m 07.47s	42° 08′33.4″	5.6″ × 4.1″	135°	−4.5	2.7	9±2	0.2±0.1
11	20h 37m 08.74s	42° 08′57.7″	3.6″ × 3.2″	96°	−3.9	2.0	10±4	0.2±0.2

[1] Determined from 2-dimensional gaussian fits to the integrated intensity map of the $2_0 \rightarrow 1_0A^+$ methanol transition. The size is uncorrected for the synthesised beam.
[2] Errors only include the statistical errors on the fit.
[3] Clump 2 corresponds to the maximum seen in the $2_1 \rightarrow 1_1E$ close to the maser, and the results are given for the 2-dimensional gaussian fit performed on the integrated intensity map of this transition.

Table 4. Methanol line parameters towards MM1

Transition	T_b K	v_{lsr} kms^{-1}	Δv kms^{-1}
$2_0 \rightarrow 1_0A^+$	8.6±0.7	-3.8 ± 0.1	4.0 ± 0.2
$2_{-1} \rightarrow 1_{-1}E$	8.8±0.7	-3.6 ± 0.1	3.6 ± 0.2
$2_0 \rightarrow 1_0E$	9.3±0.7	-3.4 ± 0.1	3.4 ± 0.2
$2_1 \rightarrow 1_1E$	7.4±0.7	-3.5 ± 0.1	3.3 ± 0.2

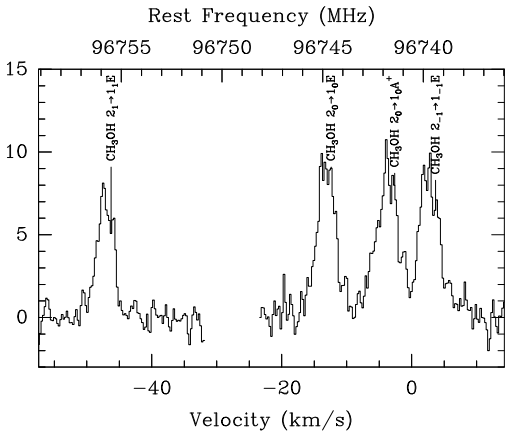

Fig. 7. Spectrum of the four methanol transitions towards MM1. The spectrum is an average over a box of 1″ around the continuum position from Table 1. The ordinate is brightness temperature (1 K = 91 mJy/beam).

wards Orion-KL are similar line ratios observed (see Fig. 2 of Menten et al. 1988). Statistical equilibrium calculations suggest in fact that densities of close to 10^7 cm^{-3} (see Fig. 9 of Menten et al. 1988) are needed to adequately populate levels such as 2_1E. This conclusion however is somewhat dependent on the observed methanol abundance and it is perhaps safer to conclude that a combination of high methanol abundance and high density are needed to explain the observations.

The methanol column density towards MM1 is therefore probably high and the value given in Table 2 may be a lower limit. Obtaining a reliable column density in this object requires a multi-transition study with high angular resolution. Another motivation for such a study is that the near equality of the peak line temperatures in Fig. 7 suggests that the lines are optically thick. Given the density in MM1 ($4\,10^7$ cm^{-3} Mangum et al. 1991), it is also likely that they are thermalised with excitation temperatures close to the kinetic temperature (at least 80 K according to Mangum et al. 1992). If this is the case, we can infer from our observed brightness temperature of order 9 K (Table 4) that the observed emission has a beam filling factor of 0.1 or less and thus is clumped on a size scale of order 1″. This may also be true for the ammonia emission (Mangum et al. 1992) which has a similar angular extent to that measured by us. The high optical depth would also have the consequence that the column density given in Table 2 is a lower limit. Thus although the methanol abundance obtained by taking the ratio of the column density given in Table 2 to the H_2 column density ($7.9\ 10^{24}$cm^{-2}, Mangum et al. 1991) is similar to dark cloud values (few 10^{-9} according to Friberg et al. 1988), it is likely that it is an underestimate by an order of magnitude or more. Indeed, one expects in a region such as DR 21(OH) to find methanol abundances similar to the estimates (10^{-7} to 10^{-6}) derived by Menten et al.(1988) for Orion and by Bachiller et al. (1995) for outflow regions. This may be true also in the case of MM1 but confirmation will require measurement of optically thin transitions of, for example, $^{13}CH_3OH$.

4.2. Comparison between thermal and maser emission

Our results towards DR 21(OH) show no clear correlation between the PM90 masers and emission in the $2_k \rightarrow 1_k$ lines. In particular, we observe no $2_k \rightarrow 1_k$ emission towards the maser DR 21(OH)-1 down to a limit of 164 mJy/beam or 1.8 K. Is this significant? One can very roughly estimate the methanol column density (and hence the $2_k \rightarrow 1_k$ intensity) required to account for the maser lines. PM90 observe a brightness temperature of 760 K and a linewidth of 0.66 km s^{-1} in a $6.5'' \times 4.4''$ beam towards DR 21(OH)-1. While we do not know the line excitation temperature $T_{\rm xm}$, a reasonable guess, based on statistical equilibrium calculations we have carried out, is that it is between -1.5 and -10. The corresponding optical depth required to explain the observed brightness temperature is of order -5 and this is liable to be an underestimate as the maser is unresolved. The methanol column density $N(CH_3OH)$ (in cm^{-2}) required to account for this optical depth can be written as (see Menten et al. 1988):

$$N(CH_3OH) \;=\; \frac{3h}{16\pi^3}(\ln 2/\pi)^{1/2}\,\frac{2Z}{\mu^2 S}\,e^{\frac{E_1}{kT_r}}\,\frac{\tau\Delta v}{(1-e^{-\frac{h\nu}{kT_{\rm xm}}})} \qquad (1)$$

Since Z, the partition function can be written as: $Z = 0.64\,T_{\rm r}^{1.5}$, we have for the 95 GHz maser line (replacing the electric dipole moment μ, the line strength S, the lower level excitation energy E_1, and the frequency ν by their respective values for this transition):

$$N(CH_3OH) \;=\; 1.6\,10^{12}\,T_{\rm r}^{1.5} e^{(79/T_{\rm r})}\,\frac{\tau\Delta v}{(1-e^{-(4.57/T_{\rm xm})})} \qquad (2)$$

In this equation, $T_{\rm r}$ is the rotation temperature approximately characterising the population distribution, τ is the maser optical depth, and Δv is the line width in km s^{-1}. Both τ and $T_{\rm xm}$ are negative for maser emission. A reasonable guess at $T_{\rm r}$ might be of the order of the level excitation or 50-100 K. Then from the above equation, we conclude that the methanol column density required to explain the observed maser emission is at least 10^{15} cm^{-2} and perhaps an order of magnitude higher. This column density however is measured along the amplification path of the maser and hence over a size-scale which may be much smaller than the PM90 beam.

On the other hand, our data place an upper limit of $\sim$1.8 K (3σ) on the intensity of e.g. $2_0 \rightarrow 1_0A^+$ emission towards DR 21 (OH)-1. Assuming this to be non-maser emission with an excitation temperature $T_{\rm xn}$ of order $T_{\rm r}$, one has for the intensity of $2_0 \rightarrow 1_0A^+$ emanating from the masing clump that:

$$T(2-1) \;=\; f_{\rm b}\,T_{\rm xn}\,(1-\exp-(\tau(2-1))) \qquad (3)$$

with

$$\tau(2-1) \;=\; 7\,10^{-13} N(CH_3OH)/(T_{\rm xn}\,T_{\rm r}^{1.5}\,\Delta v)$$

In the above, $f_{\rm b}$ is the beam filling factor of the masing region and $\tau(2-1)$ is the $2_0 \rightarrow 1_0A^+$ optical depth. One sees that, taking $T_{\rm xn} = T_{\rm r} = 100$ K and using the low optical depth limit, one has $f_{\rm b}\,N(CH_3OH) < 6\,10^{14}$ cm^{-2}. Thus for example, a maser model with beam-filling factor smaller than 0.1 (i.e angular size less than $1''$ or linear size less than 3000 AU) and CH_3OH column density 10^{16} cm^{-2} would be consistent with our upper limit on the $2_k \rightarrow 1_k$ intensity. With hindsight therefore, it is not very surprising that there are often no traces of thermal methanol in directions where $8_0 \rightarrow 7_1A^+$ emission is strong. We note however that in some cases such as DR 21-W ($\sim$ 1 K in $2_1 \rightarrow 1_1E$), there is evidence for non-maser emission associated with Class I masers. These need to be investigated more thoroughly but they do suggest that the inequalities discussed above may sometimes be equalities. If so, a more accurate determination of $f_{\rm b}$ and $N(CH_3OH)$ may be possible than from the maser emission directly.

From the above discussion, one can deduce that it is probable that the methanol column density in the maser region is of order 10^{16} cm^{-2}. For the methanol abundance range mentioned earlier, this corresponds to a hydrogen column density $10^{22} - 10^{24}$ cm^{-2}. On the other hand, statistical equilibrium calculations suggest that at densities n(H_2) $> 10^7$ cm^{-3}, the masers are quenched. It follows that the size of the masing region is likely to be above 100 AU or 30 mas at the distance of DR 21. A reasonable guess at the properties of the maser region might thus be a dense clump of size 1000 AU, density n(H_2)$\sim$ 10^6 cm^{-3} and mass $\sim$ 0.01 $M_\odot$. This estimate has large uncertainties but may be useful as a guide to future work.

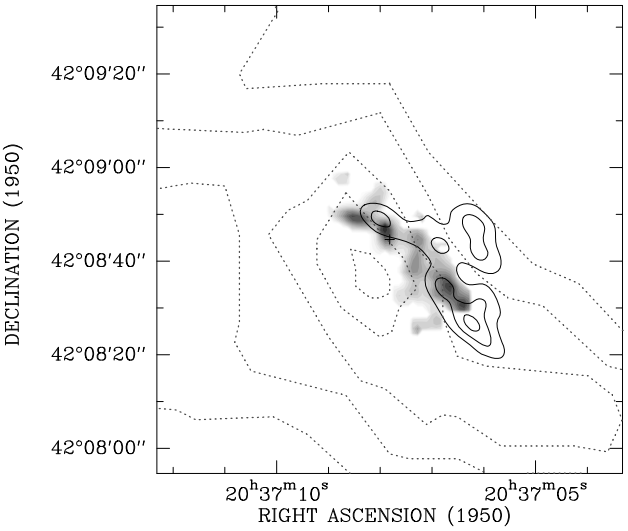

Fig. 8. Methanol, CS and vibrationally excited H_2 emission in DR 21-W. The methanol emission is shown by the same grey-scale map as in Fig. 6. Solid contours represent CS(2–1) emission (PM90) and dashed contours represent the $2.2\mu m$ emission from shock-excited H_2 (Garden et al. 1986).

4.3. Comparison between methanol and other molecular lines in DR 21-W

Fig. 8 shows our map of $2_0 \rightarrow 1_0A^+$ emission towards DR 21-W compared with contours of CS(2–1) emission(PM90) and with

vibrationally excited H_2. The latter is thought to trace gas shocked by the impact of the DR 21 outflow (Garden et al. 1991, Garden and Carlstrom 1992) on the ambient medium. One sees that methanol appears to be sandwiched between the ambient medium as represented by CS and the hot shocked gas observed in molecular hydrogen emission. This suggests that the methanol abundance is higher at the "front" between outflow and shock than in the ambient gas. Thus a scenario where the methanol is produced in the front where the flow impinges on the high density molecular clump seems possible.

We estimate that the CH_3OH column density averaged over a $3.1'' \times 3.8''$ beam varies between 0.2 and 1.1 10^{15} cm^{-2} over our map. The higher value is found towards the $2_1 \rightarrow 1_1$E clump associated with the maser (Table 3). The peak H_2 column densities in the DR 21 outflow lobes have been estimated by Garden & Carlstrom (1992) to have values between 5 10^{22} and 1 10^{23} cm^{-2} based upon their HCO^+ measurements. This depends on an uncertain estimate of the HCO^+ abundance and should only be taken as indicative. The methanol maser is located at a position offset from the HCO^+ peak and hence the beam-averaged H_2 column density may be less than 5 10^{22} cm^{-2}. We thus derive at the maser position a lower limit of 2.2 10^{-8} for the methanol abundance. Although not extremely high, this abundance is about 10 times higher than typical methanol abundances in dark clouds and quiescent clouds (Bachiller et al. 1995). Thus it is possible that, as in the case of nearby outflows, chemical processes in the shocked gas have led to enhanced methanol abundances. We note however that in this case, the observed methanol velocity and linewidth is not greatly different than that found in the ambient medium.

5. Conclusions

Our high resolution maps of $2_k \rightarrow 1_k$ methanol around the methanol masers detected in two regions of the DR 21/W 75S molecular complex show structures different from those observed in many other species. We suspect that this is due to sharp variations in the methanol abundance with enhancements in hot or shocked regions. The methanol masers detected by Plambeck and Menten (1990) do not in general coincide with peaks on our maps although there are exceptions to this (most interesting being a peak in $2_1 \rightarrow 1_1$E emission towards DR 21-W). We consider the significance of this and conclude that a plausible but certainly not unique model is one in which the masers form in structures of size roughly 1000 AU and mass 0.01 $M_\odot$. Higher angular resolution measurements of the masers are clearly warranted.

A surprising by–product of our observations was the realisation that the methanol column density towards the submm continuum source DR 21 MM1 is extremely high (at least 3 10^{16} cm^{-2} but perhaps much more). Analysing this properly requires interferometric observation of higher excitation methanol lines as single dish spectra are confused by surrounding material.

Another interesting result is the stratification of the molecular emission in the shock front of the western lobe of the outflow; the thermal methanol appears to be "sandwiched" between the molecular outflow and the dense surroundings as traced by CS. We take this as another confirmation that the methanol abundance is enhanced in outflow shock fronts. This probably occurs due to release of methanol formed in a dust grain ice mantle and released by sputtering in the outflow shock.

Acknowledgements. We would like to thank R.Bachiller and K.M.Menten for their helpful comments on the text. S.L. thanks the Max-Planck Institut für Radioastronomie and the Spanish DGICYT (grant number PB93-04) for their partial support during this work.

References

Bachiller, R., Liechti, S., Walmsley, C.M., Colomer, F., 1995, A&A, 295, L51
Batrla, W., Menten, K.M., 1988, ApJ, 329, L117
Dickel, H.R., Wendker, H.J., Bieritz, J.H., 1969 in "Proc. of IAU Symp. 38, The spiral structure of our Galaxy", p.213, Ed. W. Becker, G. Contopoulos, Reidel, Dordrecht.
Dickel, H.R., Ho, P.T.P., Wright, M.C.H., 1985, ApJ, 290, 256
Friberg P., Madden S.C., Hjalmarson A, Irvine W.M., 1988, A&A, 195, 281
Garden, R.P., Hayashi, M., Gatley, I. et al., 1991, ApJ, 374, 540
Garden, R.P., Carlstrom, J.E., 1992, ApJ, 392, 602
Guilloteau, S., Delannoy, J., Downes, D. et al., 1992, A&A, 262, 633
Gottlieb, C.A., Ball, J.A., Gottlieb, E.W., Dickinson, D.F., 1979, ApJ, 227, 422
Johnston, K.J., Henkel, C., Wilson, T.L., 1984, ApJ, 285, L85
Liechti, S., Wilson, T.L., 1996, A&A, in press.
Mangum, J.G., Wootten, A., Mundy, L.G., 1991, ApJ, 378, 576
Mangum, J.G., Wootten, A., Mundy, L.G., 1992, ApJ, 388, 467
Menten, K.M., Walmsley, C.M., Henkel, C., Wilson, T.L., 1988, A&A, 198, 253
Menten, K.M., 1991, in "Skylines, Proceeding of the Third Haystack Observatory Meeting", eds. A.D. Haschick and P.T.P. Ho (San Francisco: Astr. Soc. Pac.), p. 119.
Norris, R.P., Booth, R.S., Diamond, P.J. et al., 1982, MNRAS, 201, 191
Plambeck, R.L., Menten, K.M., 1990, ApJ, 364, 555
Richardson, K.J., Sandell, G., Cunningham, C.T. et al., 1994, A&A, 286, 555
Roelfsema, P.R., Goss, W.M., Geballe, T.R., 1989, A&A, 222, 247
Steppe, H., Paubert, G., Sievers, A. et al., A&AS, 102, 611
Woody, D.P., Scott, S.L., Scoville, N.Z. et al., 1989, ApJ, 337, L41

This article was processed by the author using Springer-Verlag LaTeX A&A style file *L-AA* version 3.